Supporting Information

Development and application of a Raster-spot model in Galvo-*fs*LA-ICP-MS for precise trace-element and U-Pb isotopic analysis

Deng-Fei Duan[*a], Qi-Rong Duan[a#], Hai-Long, Cao[a], Chang-Xin Yin[a], Ao-Di, Lu[b], **Jing Wu**[*a], Xiao-Ping Xia[a], Feng Guo[a], Yan-Jie Tang[a], Yue Wu[a], Ping Yang[a], Jun-Qin Wang[c], Ling Yu[a], Wen-Ting Yang[a]

a YU-CUGW Joint Research Center on Deep Earth and Surface Dynamic Coupling, College of Resources and Environment, Yangtze University, Wuhan 430100, PR China

b Shanghai Chemlab Instrument Co., Ltd., Wuhan 430074, China

c China University of Geoscience (Beijing), Beijing 100083, China

Research Assistant

* Corresponding authors

Table of Contents

Experimental

Reagents and reference Materials

This experiment employed a series of mineral reference materials to evaluate the performance of a newly developed galvanometer femtosecond laser system utilizing a raster-spot model. These reference materials encompass various minerals, including zircon, apatite, monazite, rutile, and allanite. Their U-Pb ages have been precisely determined by isotope dilution thermal ionization mass spectrometry (ID-TIMS), and they exhibit a wide range of U contents, which makes them suitable for validating the analytical precision and accuracy of the laser ablation system.

For age calibration, corresponding external standards were applied to each mineral: 91500 for zircon, MAD2 for apatite, RW-1 for monazite, RMJG for rutile, and AMK for allanite. During the analytical session, each external standard was inserted and measured twice after every 5-10 unknown samples to correct for elemental fractionation and instrumental mass bias.

Trace element determinations and in-situ zircon U-Pb dating

Prior to laser connection, the stability and sensitivity of the ICP-MS were optimized using a tuning solution (containing ^{6}Li, ^{59}Co, ^{89}Y, ^{115}In, and ^{205}Tl at 1 ng·g^{-1}) in solution nebulizer mode. Laser parameters, including energy, frequency divider (F), Mark-speed, Jump-speed, number of layers, number of lines ablated per times (n), interval time, and spot size, were adjusted according to the specific samples. n define the number of scanning lines per sub-cycle within a single layer, while interval time refers to the pause between consecutive sub-cycles. During laser ablation, the sample cell was continuously flushed with high-purity helium, and the resulting aerosol was mixed with argon and nitrogen. In laser sampling mode, helium (99.999 % purity, 0.4 L·min^{-1} for raster-spot model; 0.58 L·min^{-1} for frequency-divider model) was used as the ablation carrier gas to enhance aerosol transport efficiency and signal intensity, while nitrogen was introduced to further improve signal sensitivity. The aerosol passed through a signal-smoothing device before entering the ICP-MS[1]. Each measurement sequence consisted of three stages: approximately 15 s of gas blank acquisition with the laser off, about 50 s of sample signal acquisition with the laser on, and a 30 s washout period. Calibration was performed using NIST SRM 610, GSE-2G, and GSC-2G as external standards, while reference glasses OA-1, OH-1, OJY-1, BHVO-2G, and NKT-1G were analyzed as unknown samples. Silicon (^{29}Si) was used as the internal standard, with recommended values obtained from the GeoRem database (http://georem.mpch-mainz.gwdg.de). Detailed parameters and conditions of the instrument listed in Table S1 and Table S2.

For U-Pb dating analysis, the sample cell and gas pathway were purged with high-purity argon (Ar) and helium (He) prior to measurement to reduce common lead (Pb) contamination. The total acquisition time for each analysis point was approximately 90 s, consisting of three stages: about 15 s of gas blank acquisition with the laser off, about 45 s of sample signal acquisition with the laser on, and a subsequent 30 s washout period. Laser ablation was performed using the Raster-spot model. The ablated aerosol was carried out of the ablation cell by helium (flow rate ~0.4 $L \cdot min^{-1}$), then mixed with argon (~1.0 $L \cdot min^{-1}$) and nitrogen (~0.004 $L \cdot min^{-1}$), homogenized through a signal-smoothing device[1], and finally introduced into the inductively coupled plasma mass spectrometer (ICP-MS) for analysis. The data were calibrated using corresponding reference materials. Age uncertainties and the concordance MSWD were calculated using the IsoplotR online module. Detailed parameters and conditions of the instrument listed in Table S1; Table S2 and Table S3

Table S1 Instruments parameters for trace elements analysis and U-Pb dating by the Galvo-fsLA-ICP-MS.

Laser ablation system	Galvo-fsLA (Raster-spot model)
Model	GenesisGEO
Laser	femtosecond
Power	3.3 W
Wavelength	343 nm
Pulse width	259 fs
Repetition rate of the laser	1000 KHz
Sampling mode	Raster-spot ablation
Carrier gas	He: ~0.4 L min^{-1}
Sample gas	Ar: ~1.0 L min^{-1}; N_2: ~0.004 L min^{-1}
Background	15s
Wash-out time	30s
Mass spectrometer	Agilent 8900
RF power	~1500 W
Cool gas	Ar: ~15 L min^{-1}
Sample introduction	Dry transport via 6 mm ID &1 m length PTFE tubing
Interface cone	Ni
Data acquired	Time-resolved analysis
Detector mode	Pulse counting
Mass acquired	^{7}Li, ^{9}Be, ^{23}Na, ^{24}Mg, ^{27}Al, ^{29}Si, ^{43}Ca, ^{47}Ti, ^{51}V, ^{57}Fe, ^{59}Co, ^{60}Ni, ^{63}Cu, ^{66}Zn, ^{71}Ga, ^{85}Rb, ^{88}Sr, ^{90}Zr, ^{93}Nb, ^{95}Mo, ^{121}Sb, ^{133}Cs, ^{137}Ba, ^{139}La, ^{140}Ce, ^{141}Pr, ^{146}Nd, ^{147}Sm, ^{153}Eu, ^{157}Gd, ^{159}Tb, ^{163}Dy, ^{165}Ho, ^{166}Er, ^{169}Tm, ^{172}Yb, ^{175}Lu, ^{178}Hf, ^{182}W, ^{206}Pb, ^{207}Pb, ^{208}Pb, ^{232}Th, ^{238}U

Table S2 Laser ablation parameters for trace element analysis and U-Pb dating, Divider-frequency divider

A. Trace element analysis: model comparison on glass reference materials

Model	Attenuator A×B	Energy (μJ)	Divider	Spot Size (μm)	MarkSpeed (μm/s)	JumpSpeed (μm/s)	LineInterval (μm)	Layers	n	MarkInterval (ms)
Frequency-divider model	45% × 45%	~0.200	100	34.5	40000	1000000	1.5	54	—	1800
Raster-spot model	45%×45%	~0.200	10	34.5	150000	1000000	1.5	24	12	1000

Note: A total of 42 isotopes were measured, each with a dwell time of 0.006 s.

B. U-Pb dating: mineral-specific laser parameters (Raster-spot model only)

Mineral	Attenuator A×B	Energy (μJ)	Divider	Spot Size (μm)	MarkSpeed (μm/s)	JumpSpeed (μm/s)	LineInterval (μm)	Layers	n	MarkInterval (ms)
Zircon	50% × 50%	~ 0.252	10	8.4	110000	1000000	1.2	16	4	700
				10.8	120000	1000000	1.2	20	5	800
				21	150000	1000000	1.5	16	5	900
				30	150000	1000000	1.5	28	7	500
			40	21	37500	1000000	1.5	26	5	600
				30	37500	1000000	1.5	28	7	500
Apatite	46% × 46%	~ 0.210	10	15	150000	1000000	1.5	16	11	1200
				30	150000	1000000	1.5	12	7	1100
				39	150000	1000000	1.5	12	9	1100
			40	39	37500	1000000	1.5	12	9	1100
Rutile	30% × 30%	~ 0.083	10	19	150000	1000000	1	16	10	800
				30	150000	1000000	1.5	28	7	500
Allanite	45% × 45%	~ 0.200	10	13.2	120000	1000000	1.2	12	4	1200
	30% × 30%	~ 0.083	40	30	37500	1000000	1.5	20	7	750
Titanite	40% × 40%	~ 0.156	40	30	37500	1000000	1.5	14	7	1000
Monazite	34% × 34%	~ 0.109	40	13.5	37500	1000000	1.5	8	2	1000

Note: A total of 5 isotopes were measured, as listed below: ^{206}Pb, ^{207}Pb, ^{208}Pb, ^{232}Th, ^{238}U

C. Dwell times of isotopes for U-Pb dating of different minerals (Raster-spot model only)

Mineral	Spot Size (μm)	Dwell Time (s)	Mineral	Spot Size (μm)	Dwell Time (s)
Zircon	10.8	0.03 s for ^{206}Pb; 0.06 s for ^{207}Pb; 0.006 s for ^{208}Pb and ^{232}Th; 0.01 s for ^{238}U	Zircon	8.4, 21, 30	0.015 s for ^{206}Pb and ^{208}Pb; 0.03 s for ^{207}Pb; 0.01 s for ^{232}Th and ^{238}U
Apatite	15, 30, 39	0.03 s for ^{206}Pb, ^{207}Pb and ^{238}U; 0.006 s for ^{208}Pb and ^{232}Th	Apatite	22.8	0.004 s for ^{206}Pb, ^{208}Pb and ^{232}Th; 0.02 s for ^{207}Pb; 0.007 s for ^{238}U
Rutile	19, 30	0.03 s for ^{206}Pb, ^{207}Pb, ^{208}Pb ^{232}Th and ^{238}U	Allanite	13.2, 30	0.03 s for ^{206}Pb, ^{207}Pb and ^{238}U; 0.003 s for ^{208}Pb and ^{232}Th
Titanite	30	0.015 s for ^{206}Pb and ^{208}Pb; 0.03 s for ^{207}Pb; 0.01 s for ^{232}Th and ^{238}U	Monazite	13.5	0.015 s for ^{206}Pb; 0.02 s for ^{207}Pb and ^{208}Pb; 0.015 s for ^{232}Th and ^{238}U

Table S3 U-Pb dating: mineral-specific laser parameters (Frequency-divider model), Divider-frequency divider

Mineral	Attenuator A×B	Energy (μJ)	Divider	Spot Size (μm)	MarkSpeed (μm/s)	JumpSpeed (μm/s)	LineInterval (μm)	Layers	MarkInterval (ms)
Zircon	47% × 47%	~ 0.220	200	15	60000	1000000	2	320	250
	50% × 50%	~ 0.252	200	15	60000	1000000	2	320	250
	46% × 46%	~ 0.210	40	20	200000	1000000	2	200	500
	50% × 50%	~ 0.252	120	20	60000	1000000	3	320	250
	47% × 47%	~ 0.220	200	20	60000	1000000	2	350	250
	50% × 50%	~ 0.252	200	20	60000	1000000	2	320	250
	47% × 47%	~ 0.220	40	30	400000	1000000	2	200	500
	55% × 55%	~ 0.302	40	30	200000	1000000	2	200	500
	50% × 50%	~ 0.252	120	30	60000	1000000	3	320	250
	47% × 47%	~ 0.220	200	30	60000	1000000	2	350	250

PowerPoint document Comparison of SEM images of ablation craters obtained on NIST SRM 610 using the Dense-fill model, Frequency-divider model, and Raster spot model under different parameter conditions (laser conditions: energy: ~ 0.252 μJ; mark-speed: 10^5 μm/s; jump-speed: 10^6 μm/s; line interval: 1 μm; mark interval: 1000 ms; **number of lines ablated per times (n)for Raster-spot model: 3 (5μm), 8 (15 μm), 7 (20 μm), 11 (32 μm), 15 (44 μm), 18 (53 μm), 36 (179 μm)**

Figure. S1 Transient signal intensity of ^{7}Li, ^{9}Be, ^{23}Na, ^{24}Mg, ^{27}Al, ^{43}Ca, ^{47}Ti, ^{51}V, ^{57}Fe, ^{59}Co, ^{60}Ni, ^{71}Ga, ^{85}Rb, ^{88}Sr, ^{90}Zr, ^{93}Nb, ^{95}Mo, ^{121}Sb, ^{133}Cs, ^{137}Ba, ^{139}La, ^{140}Ce, ^{141}Pr, ^{146}Nd, ^{147}Sm, ^{153}Eu, ^{157}Gd, ^{159}Tb, ^{163}Dy, ^{165}Ho, ^{166}Er, ^{169}Tm, ^{172}Yb, ^{175}Lu, ^{178}Hf, and ^{182}W in NIST SRM 610 obtained using the Dense-fill model (laser conditions: spot size: 34.5 μm; energy: ~ 0.200 μJ; frequency divider: 1; mark-speed: 10^{6} μm/s, jump speed: 10^{6} μm/s, line interval: 1 μm, layers: 100; mark interval: 1000 ms), Frequency-divider model and Raster-spot model. Parameters for Frequency-divider model and Raster-spot model were listed in Table S2A

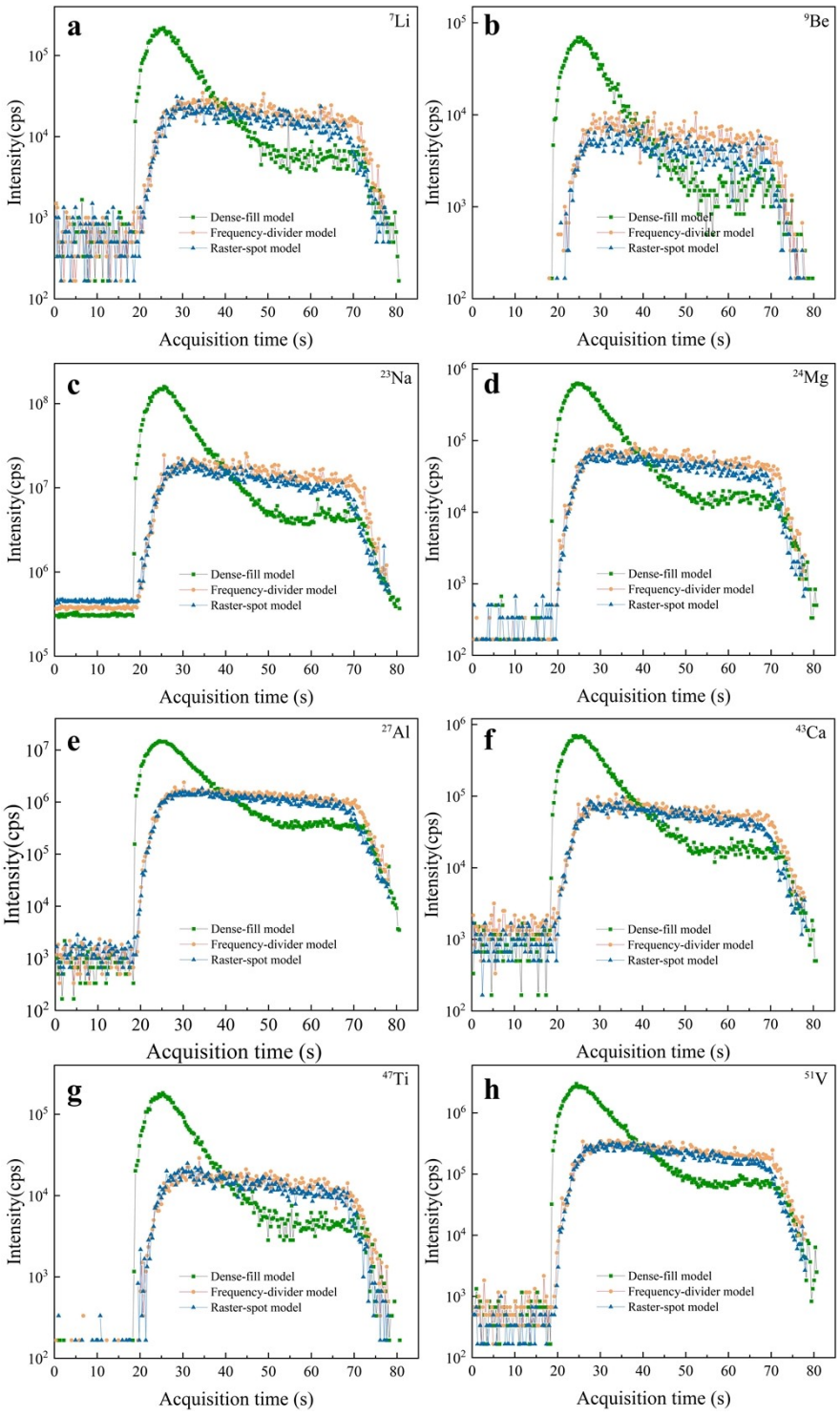

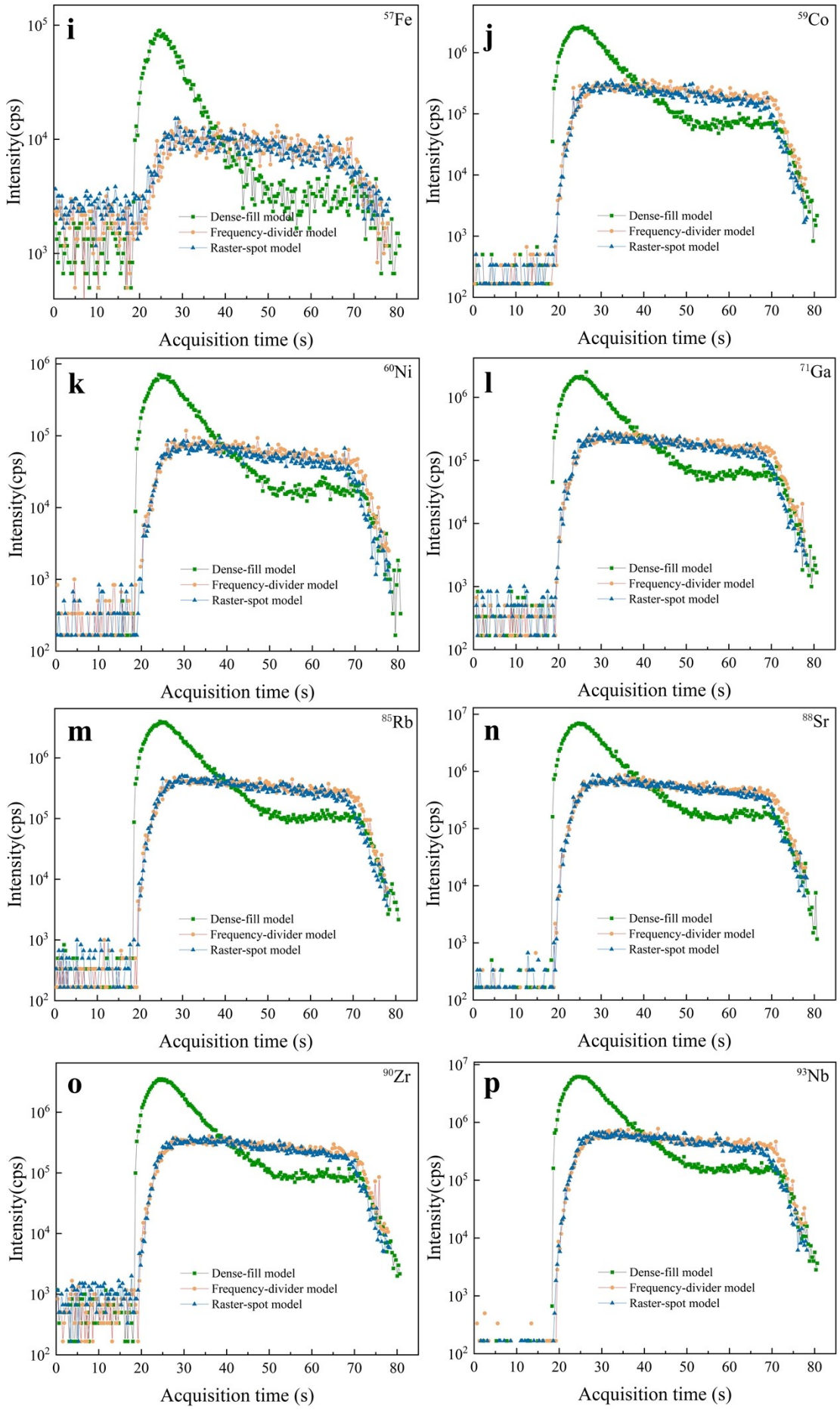
i
^{57}Fe
j
^{59}Co
k
^{60}Ni
l
^{71}Ga
m
^{85}Rb
n
^{88}Sr
o
^{90}Zr
p
^{93}Nb
Intensity(cps)
Acquisition time (s)
Dense-fill model
Frequency-divider model
Raster-spot model

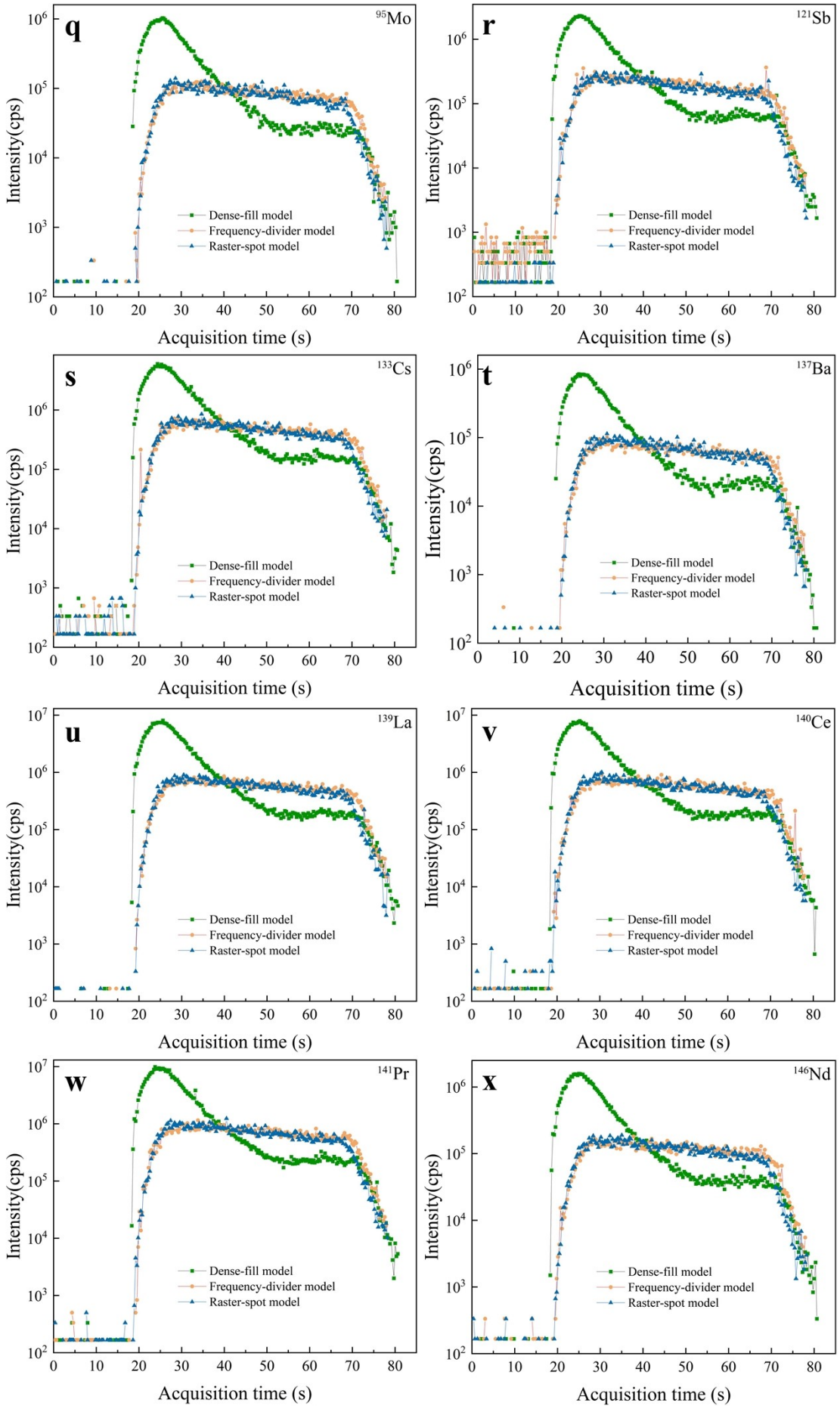
q
^{95}Mo
r
^{121}Sb
s
^{133}Cs
t
^{137}Ba
u
^{139}La
v
^{140}Ce
w
^{141}Pr
x
^{146}Nd
Intensity(cps)
Acquisition time (s)
Dense-fill model
Frequency-divider model
Raster-spot model

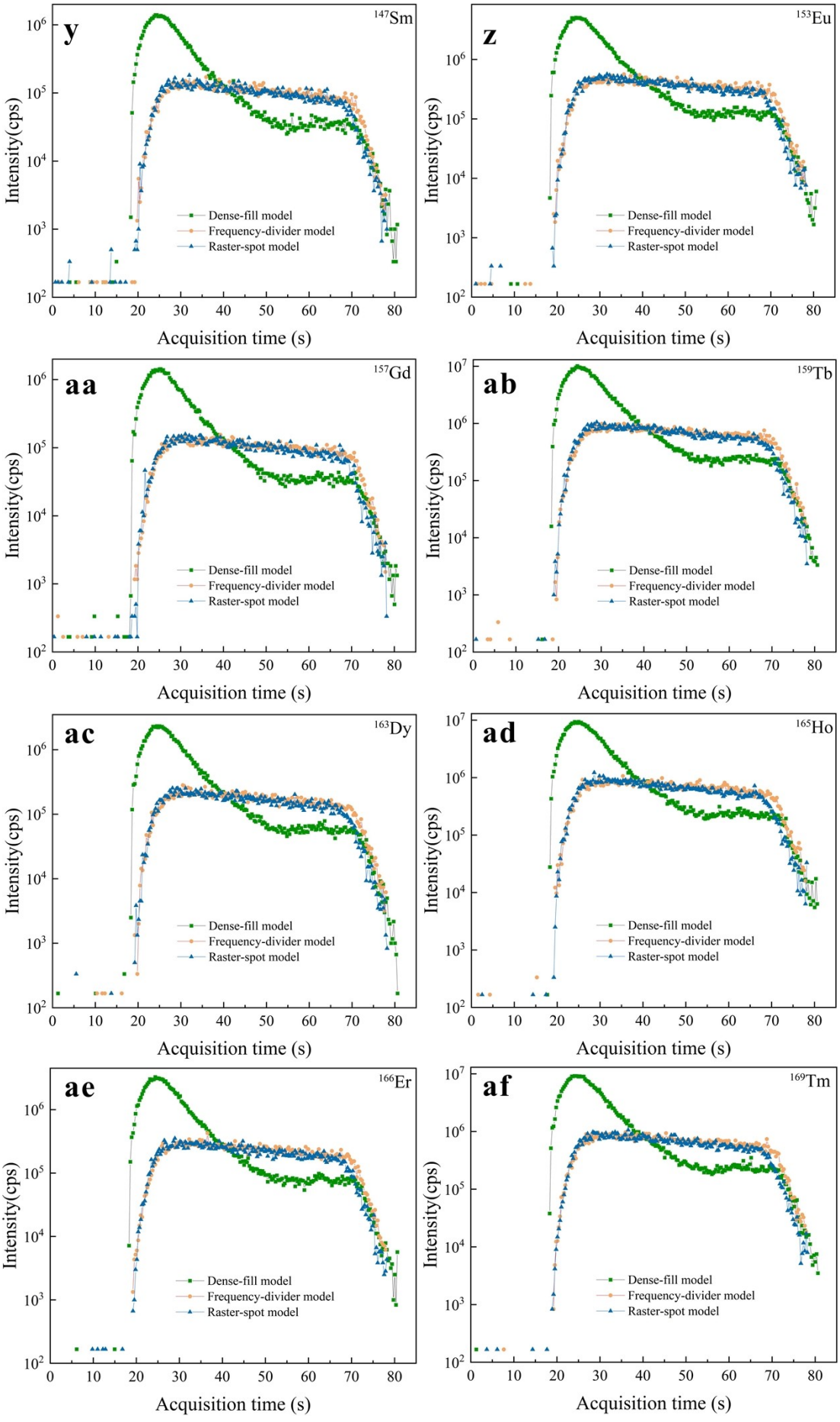
y
147Sm
z
153Eu
aa
157Gd
ab
159Tb
ac
163Dy
ad
165Ho
ae
166Er
af
169Tm
Intensity(cps)
Acquisition time (s)
Dense-fill model
Frequency-divider model
Raster-spot model

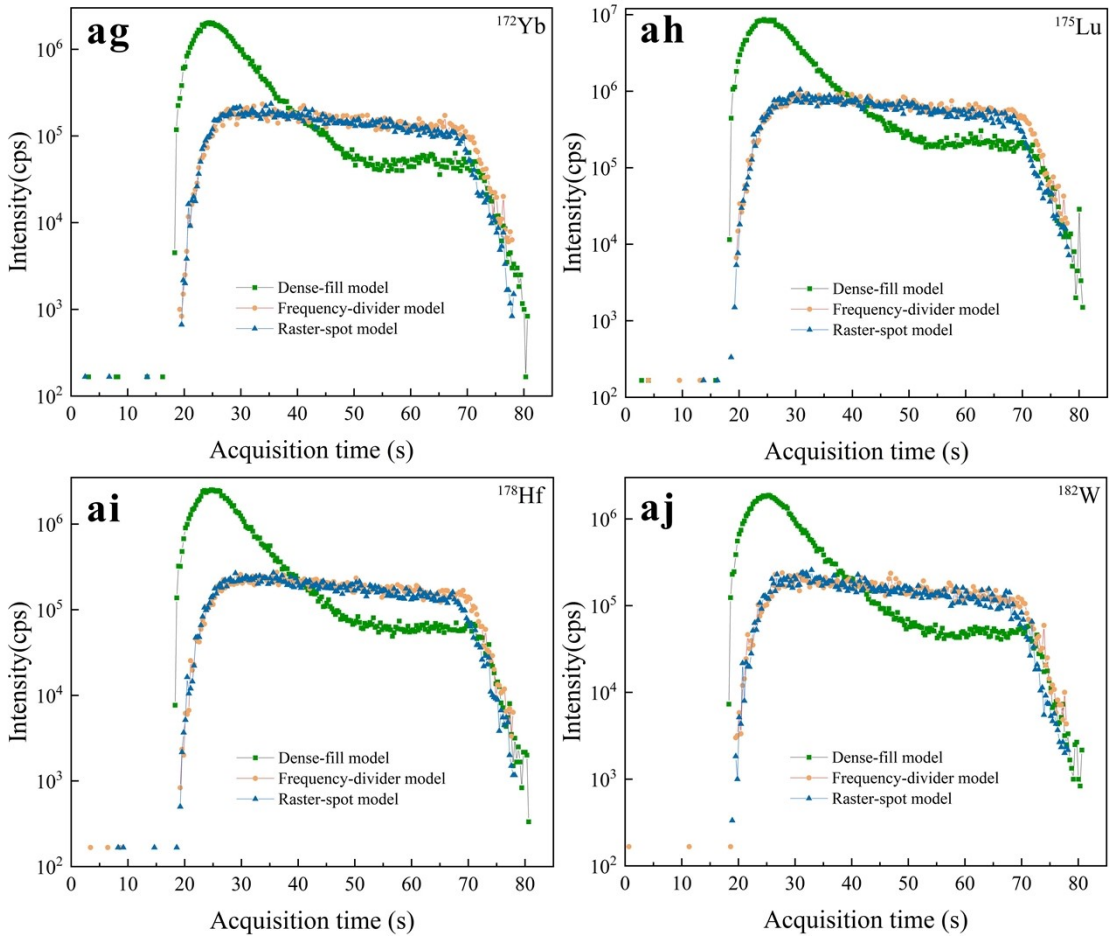
ag
^{172}Yb
ah
^{175}Lu
ai
^{178}Hf
aj
^{182}W
Intensity(cps)
Acquisition time (s)
Dense-fill model
Frequency-divider model
Raster-spot model

Figure. S2 Long-term measurements of reference materials during U-Pb dating, with laser parameters listed in Table S2B, C and Table S3

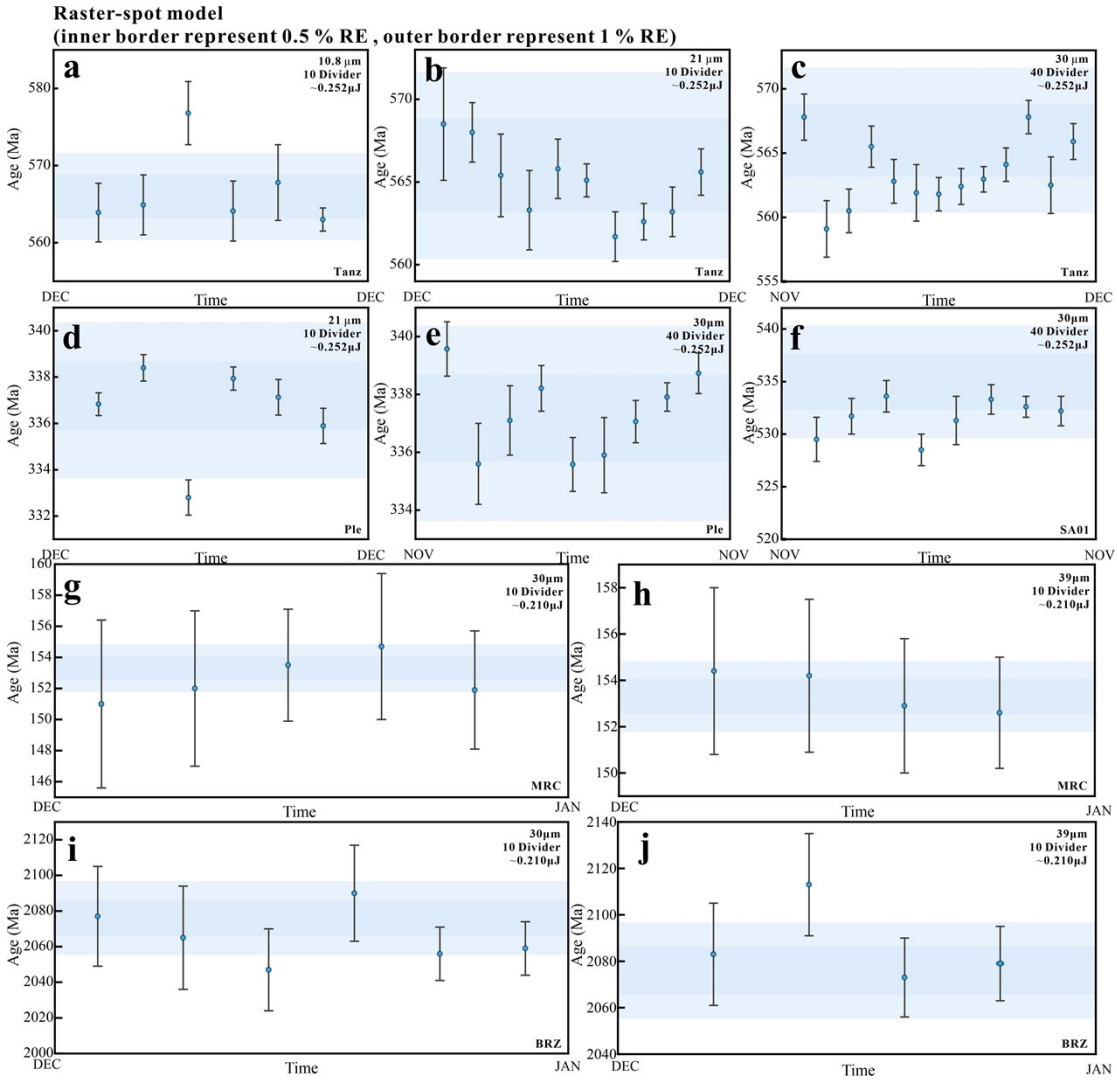

Frequency-divider model
(inner border represent 1 % RE , outer border represent 2 % RE)

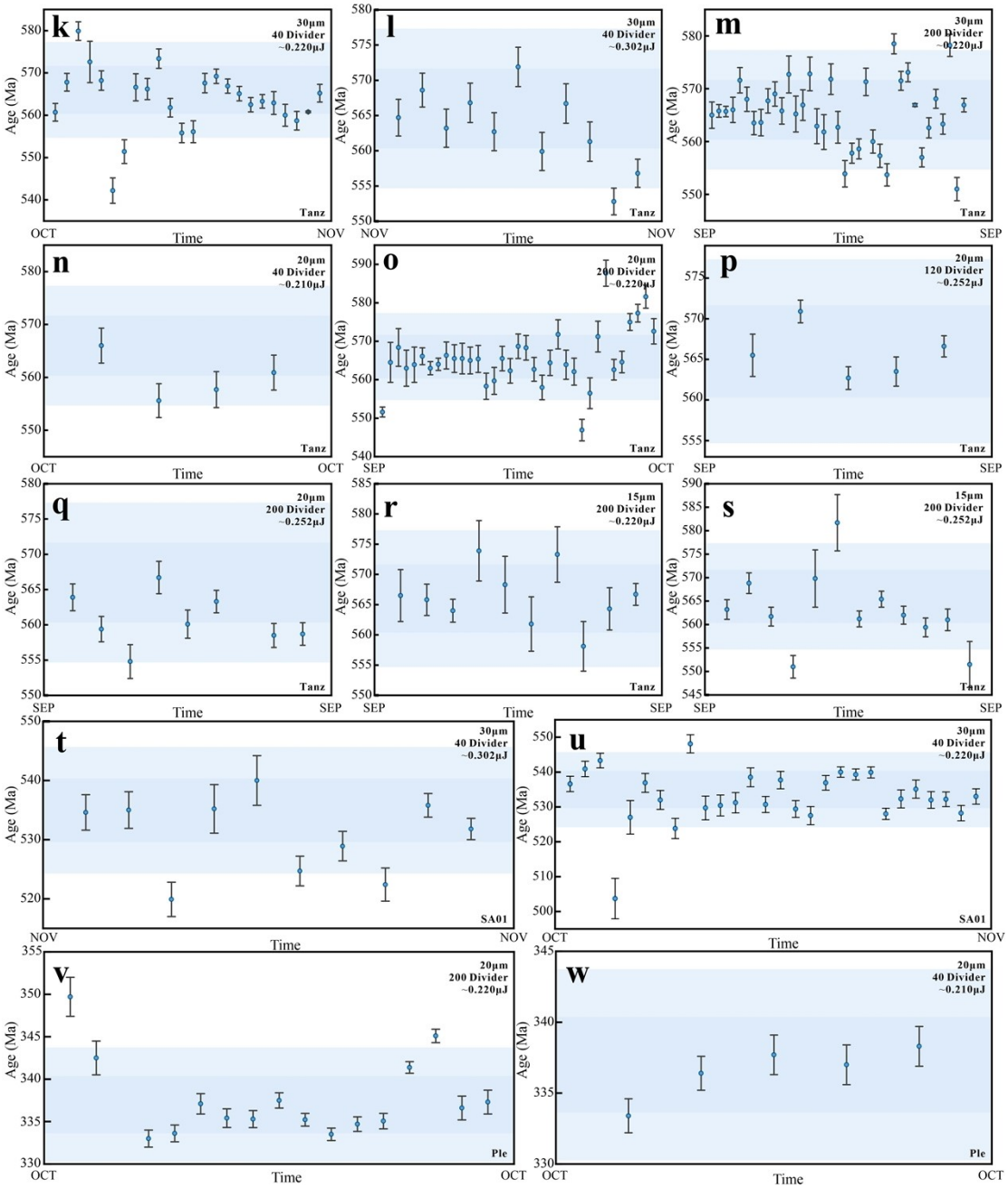

Figure. S3 Concordia diagrams of U-Pb dating for Zircon (a-f), Apatite (g-i), Allanite (j-k) and monazite (l) obtained using the Raster-spot model

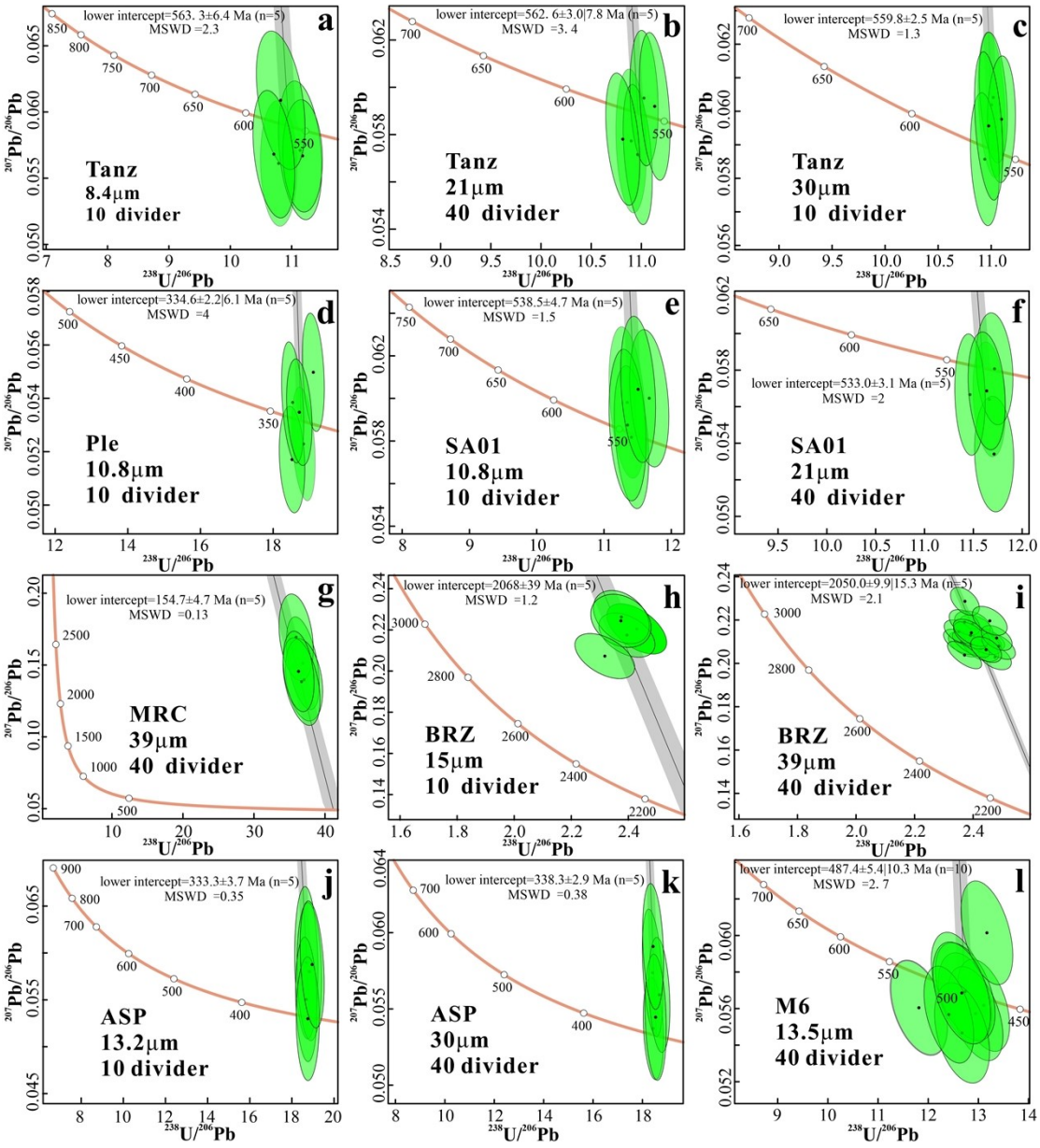

Reference

(1) Hu, Z., Zhang, W., Liu, Y., Gao, S., Li, M., Zong, K., ... & Hu, S. (2015). “Wave” signal-smoothing and mercury-removing device for laser ablation quadrupole and multiple collector ICPMS analysis: application to lead isotope analysis. Analytical Chemistry, 87(2), 1152-1157.